energies

MDPI

Review

PSO-Based Model Predictive Control for Load Frequency Regulation with Wind Turbines

Wei Fan [1], Zhijian Hu [2] and Veerapandiyan Veerasamy [2,*]

[1] School of Electrical Engineering, Anhui Polytechnic University, Wuhu 241000, China
[2] School of Electrical and Electronic Engineering, Nanyang Technological University, Singapore 639798, Singapore
* Correspondence: veerapandiyan.v@ntu.edu.sg

Abstract: With the high penetration of wind turbines, many issues need to be addressed in relation to load frequency control (LFC) to ensure the stable operation of power grids. The particle swarm optimization-based model predictive control (PSO-MPC) approach is presented to address this issue in the context of LFC with the participation of wind turbines. The classical MPC model was modified to incorporate the particle swarm optimization algorithm for the power generation model to regulate the system frequency. In addition to addressing the unpredictability of wind turbine generation, the presented PSO-MPC strategy not only addresses the randomness of wind turbine generation, but also reduces the computation burden of traditional MPC. The simulation results validate the effectiveness and feasibility of the PSO-MPC approach as compared with other state-of-the-art strategies.

Keywords: wind turbines; load frequency control; particle swarm optimization; model predictive control

Citation: Fan, W.; Hu, Z.; Veerasamy, V. PSO-Based Model Predictive Control for Load Frequency Regulation with Wind Turbines. *Energies* **2022**, *15*, 8219. https://doi.org/10.3390/en15218219

Academic Editor: Adrian Ilinca

Received: 10 October 2022
Accepted: 2 November 2022
Published: 3 November 2022

1. Introduction

Load frequency control (LFC) is one of the significant ancillary services in the power system. It is used to maintain the frequency of the system through active power output variation of generator sets. When load disturbances of the power system vary, the nominal frequency fluctuates accordingly, resulting in a poor load-generation balance [1,2]. The load frequency controllers of conventional generator sets, such as the proportional integral (PI) controller [3,4], robust controller [5,6], and fuzzy controller [7–9], offer effective ways to control the area control error (ACE) of the system. With the development of the world economy and the improvement of people's material living standards, the power supply demand is increasing day by day, as is the power supply gap [10]. However, the traditional thermal power supply mode releases significant amounts of pollution into the environment, making environmental and economic sustainability hard to achieve. Thus, the development of "carbon peak and carbon neutrality" increases the renewable energy (RE) power supply, which will help balance the load demand in the new era. Wind energy generation is one of the predominant sources of renewable energy. However, the increasing penetration of wind turbines will change the way in which the frequency of power grids is controlled, as compared to the conventional approaches [11].

In recent decades, the power generation model with wind turbine integration has been widely studied. Due to its intrinsic uncertainty and the large fluctuations caused by the stochastic wind velocity, there are significant challenges associated with wind turbines in relation to the stability and controllability of power grids. Through the application of genetic and fuzzy logic controllers in LFC, the influence of doubly fed induction generator (DFIG) systems on LFC was evaluated [12]. At present, the wind power model is widely used for DFIG systems. By combining the original dynamic model of power systems with the dynamic model of wind turbines, the state space equation for LFC with the participation of wind turbines was deduced [13]. A model reference adaptive controller (MRAC) was applied to modify the controller gains during sudden load perturbation. Further, to

improve its efficacy, a neural network with MRAC was utilized to minimize the error signal in the conventional MRAC [14]. However, these two kinds of schemes for the parameter optimization process are relatively complex, and have a great computational burden. When the region has multiple hybrid power systems (HPS), the interconnected HPS model runs in different combinations. A Hankel model order reduction method was used to analyze the stability of the model, and a particle swarm optimization-gravity search algorithm (PSO-GSA) was employed. In this study, the integral absolute error (IAE) of the control error was used as the optimization cost function to optimize the gain of the controller and realize the frequency response of the system [15]. The control strategy considers the traditional hybrid power generation mode and does not introduce a new energy generation mode. Considering the load variation of RE and weather intermittency, a hybrid mirror group optimization gravity search algorithm based on chaos search was proposed. By minimizing the absolute error of integration time of an HPS, the PID control parameters of LFC were obtained. Through comparison and a stability analysis, the effectiveness of this strategy was verified [16]. This method has a large amount of computation and optimization parameters, which increases the burden of communication and operation. On the other hand, plug-in electric vehicles (PEVs) can be regarded as manageable energy storage systems with the ability to respond quickly to load disturbances, and adding a number of PEVs to LFC is an effective way to achieve rapid regulation. In [17], a distributed LFC strategy was used to integrate resilient distributed frequency estimation schemes based on credibility. The proposed credibility-based distributed frequency estimation scheme was verified under various communication topologies, and the simulation results of a four-area power system show that the proposed distributed LFC strategy can quickly regulate the frequency after detecting and isolating the compromised PEVs. According to literature [18], machine learning and deep learning control strategies have the advantages of low cost, rapid response, and high accuracy, and have a long-term development prospect. Reinforcement learning has been applied to the LFC of multi-region power systems. Through the strategy of centralized learning and decentralized implementation, it was demonstrated that this method can effectively reduce the control errors caused by random frequency changes associated with load and new energy power fluctuations [19]. An artificial neural network was utilized in DFIG-based wind turbines to train the controller gains in [20], which guarantees the feasibility of controller gains even though the running condition was not included in the training set. However, this method needs a lot of experimental data and a long training time, so it may not be able to make a timely response in emergencies.

Model predictive control (MPC) was found to be an alternative approach that can effectively optimize system performance with a given model [21]. Because of its simple iteration property, the system can be processed with constraint conditions, resulting in broad applications in power grids. The exponential increase in the integration of RE resources and traditional power generation with RE resources has meant that the MPC technique has been adopted for frequency regulation in a centralized and decentralized way [22]. With the economic benefit as the starting point, a balance of power generation and power consumption was achieved under MPC, and the effectiveness was verified using a four-area system [23]. However, a large number of interconnected networks increase the burden of network communication and signal interference in neighboring areas. For this reason, a model-based internal model control was used in [24]. By combining the adaptive model in the MPC design, a new internal model controller was proposed, which can better regulate the frequency by reducing the peak response of the prime mover. In the LFC scheme, partial load fluctuations, frequency deviation, and the generation rate constraint (GRC) affected the active response of the system to a large extent; therefore, the distributed model predictive control (DMPC) strategy was proposed for processing the power system dynamic response and uncertainty [25]. However, the implementation of DMPC strategies requires the control actions to be repeatedly calculated, which consumes a lot of resources.

To enhance the efficiency and accuracy of iterative computation in MPC, a particle swarm optimization (PSO) algorithm was used in this study to optimize the iterative

process. PSO is a swarm-based evolutionary algorithm proposed by Kennedy and Eberhart [26], which optimizes the extreme points through fewer iterative calculations by reaching global minima. The optimization process of PSO does not depend on the initial position of the particle [27], but ultimately finds the optimal global solution of the objective function by finding the individual local and optimal global best in the established interval. In the traditional PID controller, the PSO algorithm is used to optimize its parameters by minimizing the absolute error of integration time (ITAE) of ACE as an objective function, which greatly improves the robustness of the system [28–30]. However, the PID controller performs poorly in complex systems with the participation of renewable energies. In addition, the PSO uses an artificial neural network (ANN) to train the optimal neural network model [31]. The mean square error of the model is used as the evaluation criterion to verify that the optimal neural network model is more effective for frequency regulation. However, the range of operating points covered by the training set greatly limits the accuracy of the method. In LFC used in conjunction with wind turbines, particle swarm optimization is used to optimize their control parameters to further reduce their fatigue compliance and improve their service life, demonstrating its powerful optimization ability [32]. However, the stability of the controller in a system where multiple power generation modes coexist remains to be discussed. While most of the exiting LFC approaches in the literature focus on PID or single MPC, these control strategies either ignore the fluctuation caused by the stochastic wind velocity or the complexity of iterative calculations. Thus, these control solutions need to be improved.

In this paper, we propose a PSO-MPC control strategy that can deal with the uncertainties of wind turbines and can enhance the computation efficiency of MPC. The main contributions are summarized as follows:

- A PSO-MPC approach is proposed for LFC with wind turbines; it can deal with the uncertainties associated with wind turbines and can explore the feasibility of integrating wind turbines into conventional power generation;
- To reduce the computational burden of implementing the MPC strategy, the particle swarm optimization algorithm is incorporated. The cost function of MPC is taken as the objective function of PSO, and the control quantity is iteratively optimized. Moreover, the influences of physical constraints, such as GRC and the governor dead zone [23], were verified using simulations. The results demonstrate that this method has a fast dynamic performance.

The arrangement of this paper is as follows. Section 2 establishes the system model, including the wind turbine model and the traditional thermal power unit model. Section 3 introduces model predictive control and cost function. Section 4 describes the particle swarm optimization algorithm and objective function formulation. Section 5 establishes the model predictive controller based on PSO tuning of its parameters. Section 6 verifies the effectiveness of the presented method using simulations. Section 7 concludes this paper.

2. System Dynamics

2.1. Simplified Wind Turbine Model

This section presents the simplified wind turbine model of a doubly fed induction generator [12]. Furthermore, the simplified model of a DFIG-based wind turbine is given in Figure 1, the operations of which are mathematically expressed as follows:

$$\dot{i}_{qr} = -\left(\frac{1}{T_1}\right) i_{qr} + \left(\frac{X_2}{T_1}\right) V_{qr} \tag{1}$$

$$\dot{w} = -\left(\frac{X_3}{2H_t}\right) i_{qr} + \left(\frac{1}{2H_t}\right) T_m \tag{2}$$

$$P_e = w X_3 i_{qr} \tag{3}$$

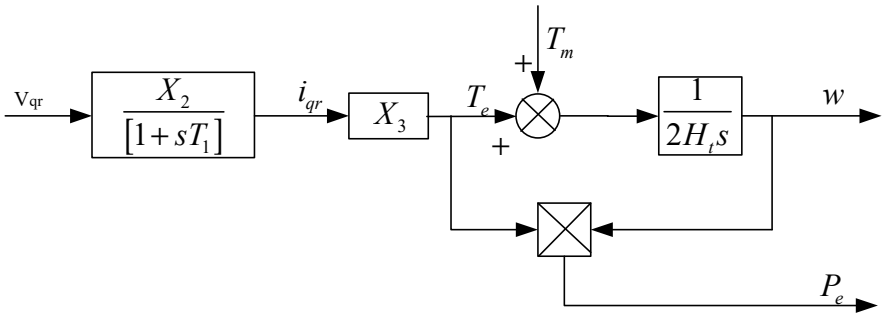

Figure 1. Simplified model of a DFIG-based wind turbine.

Via linearization, Equation (3) becomes

$$P_e = w_{opt} X_3 i_{qr} \tag{4}$$

$$T_e = i_{qs} = -\frac{L_m}{Lss} i_{qr} \tag{5}$$

The parameters of the wind turbine are defined as follows: w_{opt} is the rotor velocity at the operating point of the wind turbine; T_e is the electromagnetic torque; T_m is the mechanical power change; w is the rotor speed; P_e is the active power of the wind turbine; i_{qr} is the Q-axis component of the rotor current; V_{qr} is the Q-axis component of the rotor voltage; and H_t is the equivalent inertia constant of the wind turbine. Moreover, the main parameters for Figure 1 are given as

$$\begin{aligned} &X_2 = \tfrac{1}{R_r}, X_3 = \tfrac{L_m}{L_s} \\ &T_1 = \tfrac{L_{rr} + L_m^2 / L_{ss}}{w_s R_r} \\ &L_{ss} = L_s + L_m, L_{rr} = L_{rs} + L_m \end{aligned} \tag{6}$$

where L_m is the excitation inductance; R_r and R_s represent the rotor resistance and stator resistance, respectively; L_r and L_s represent the rotor inductance and stator inductance; L_{rr} and L_{ss} represent the mutual inductance of the rotor and stator; and w_s is the synchronous speed.

2.2. Modelling of Power System

In this section, the thermal power system model is presented, which mainly consists of three components: the secondary controller, the droop and governor control, and the turbines, as shown in Figure 2. The simulation parameters are described in Table 1, the values of which are given in the simulation.

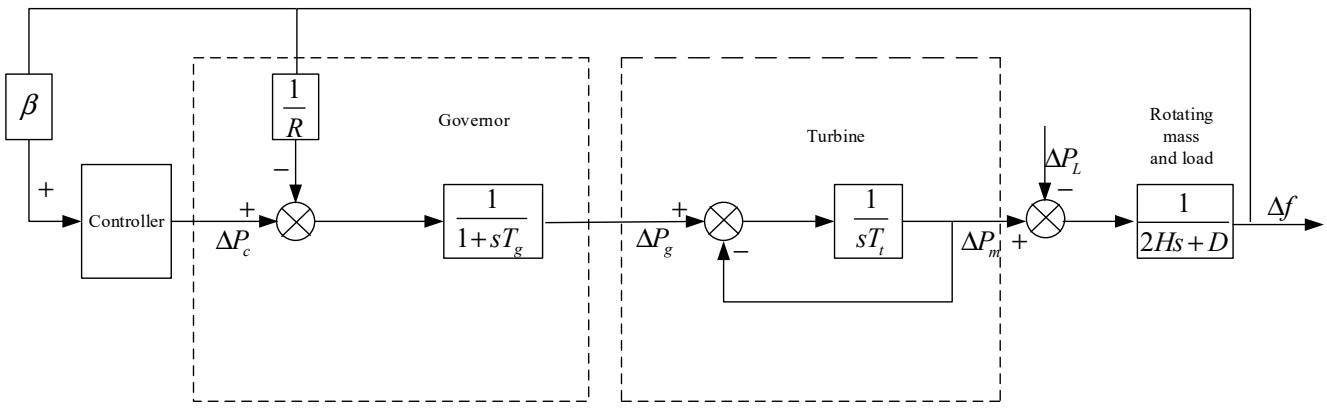

Figure 2. Dynamic model of the power system.

Table 1. Parameters of the power system.

Parameter	Physical Significance
Δf	Deviation of frequency
ΔP_m	The mechanical power change
ΔP_L	Load disturbance
ΔP_g	The governor output change
ΔP_c	Supplementary control action
R	Speed drop
T_g	Time constant of governor
T_t	Time constant of turbine
H	Equivalent inertia constant of generator
D	Equivalent damping coefficient of generator
β	Frequency bias constant
y	The system output

The overall generator-load dynamic relationship between the incremental mismatch power ($\Delta P_m - \Delta P_L$) and the frequency deviation (Δf) can be expressed as

$$\Delta \dot{f} = \left(\frac{1}{2H}\right)\Delta P_m - \left(\frac{1}{2H}\right)\Delta P_L - \left(\frac{D}{2H}\right)\Delta f \tag{7}$$

The dynamic of the governor can be expressed as

$$\Delta \dot{P}_m = \left(\frac{1}{T_t}\right)\Delta P_g - \left(\frac{1}{T_t}\right)\Delta P_m \tag{8}$$

The dynamic of the turbine can be expressed as

$$\Delta \dot{P}_g = \left(\frac{1}{T_g}\right)\Delta P_c - \left(\frac{1}{RT_g}\right)\Delta f - \left(\frac{1}{T_g}\right)\Delta P_g \tag{9}$$

Equations (1), (2), (7), (8), and (9) are simplified to obtain the state space equation of load frequency control:

$$\begin{aligned} \dot{x} &= Ax + Bu + Cz \\ y &= Dx \end{aligned} \tag{10}$$

where x represents the state of the system; u represents the control input of the system; and z represents the load disturbance.

$$x = \begin{bmatrix} \Delta P_g \\ \Delta P_m \\ \Delta f \\ \Delta i_{qr} \\ \Delta w \end{bmatrix}, u = \begin{bmatrix} \Delta P_c \\ \Delta V_{qr} \end{bmatrix}, z = \begin{bmatrix} \Delta P_L \\ \Delta T_m \end{bmatrix} \tag{11}$$

$$A = \begin{bmatrix} -\frac{1}{T_g} & 0 & -\frac{1}{RT_g} & 0 & 0 \\ \frac{1}{T_t} & -\frac{1}{T_t} & 0 & 0 & 0 \\ 0 & \frac{1}{2H} & \frac{D}{2H} & \frac{X_3 w_{opt}}{2H_t} & 0 \\ 0 & 0 & 0 & -\frac{1}{T_1} & 0 \\ 0 & 0 & 0 & -\frac{X_3}{2H_t} & 0 \end{bmatrix} \tag{12}$$

$$B = \begin{bmatrix} \frac{1}{T_g} & 0 \\ 0 & 0 \\ 0 & 0 \\ 0 & \frac{X_2}{T_1} \\ 0 & 0 \end{bmatrix}, C = \begin{bmatrix} 0 & 0 \\ 0 & 0 \\ -\frac{1}{2H} & 0 \\ 0 & 0 \\ 0 & \frac{1}{2H_t} \end{bmatrix} \tag{13}$$

$$D = \begin{bmatrix} 0 & 0 & \beta & 0 & 0 \end{bmatrix} \tag{14}$$

3. Model Predictive Control

In this section, we focus on model predictive control (MPC). MPC is an iterative optimization control algorithm. Under the given system model, it predicts the performance of the system in a certain future period to optimize the control action. Considering the power system as an example through which to better understand the model, the objective function at time k is

$$\begin{aligned} &\dot{x}(k) = Ax(k) + Bu(k) \\ &minJ(x(k), u(k)) \\ &J = \sum_{k}^{N_p-1} e(k)^T Qe(k) + u(k)^T Ru(k) + E(N)^T FE(N) \\ &e(k) = y(k) - r(k) \end{aligned} \tag{15}$$

where N_p is the prediction space of the system; Q and R are the weight parameters of the system; and $r(k)$ is the system reference input value at time k.

In the process of data collection, data are sent or received in groups through the data collector. Therefore, for the closed-loop optimal control problem, the system is modified by the following discretization method:

$$x(k+1) = Ax(k) + Bu(k) \tag{16}$$

In this model, $r(k) = 0$, $e(k)$ is the systematic error at time k; and $E(N)^T FE(N)$ is the final cost function of the system. The objective function of Formula (14) can be transformed into the following expression:

$$\begin{aligned} &\min J = \sum_{i=0}^{N_p-1} (x(k+i|k)^T Qx(k+i|k) + u(k+i|k)^T Ru(k+i|k)) \\ &\min J = X^T \widetilde{Q} X + U^T \widetilde{R} U \end{aligned} \tag{17a}$$

$$\begin{aligned} U &= \begin{bmatrix} u(k|k) & u(k+1|k) & \cdots & u(k+N_p-1|k) \end{bmatrix}^T \\ X &= \begin{bmatrix} x(k|k) & x(k+1|k) & \cdots & x(k+N_p|k) \end{bmatrix}^T \end{aligned} \tag{17b}$$

where $x(k+i\,|\,k)$, $u(k+i\,|\,k)$ represent the system state $x(k+i\,|\,k)$ predicted at time k and the control quantity $u(k+i\,|\,k)$ predicted at time k. $\widetilde{Q}$, $\widetilde{R}$ are the optimization cost coefficient matrices after appropriate augmentation transformation.

Substituting Equation (16) into Equation (17a) and simplifying it, we can obtain

$$\begin{aligned} J &= X^T \widetilde{Q} X + U^T \widetilde{R} U \\ J &= (\widetilde{A} x_k + \widetilde{B} U)^T \widetilde{Q} (\widetilde{A} x_k + \widetilde{B} U) + U^T \widetilde{R} U \\ J &= (x_k{}^T \widetilde{A}^T + U^T \widetilde{B}^T) \widetilde{Q} (\widetilde{A} x_k + \widetilde{B} U) + U^T \widetilde{R} U \\ J &= U^T H U + f^T x_k \end{aligned} \tag{18a}$$

Among them,

$$\begin{aligned} H &= \widetilde{B}^T \widetilde{Q} \widetilde{B} + \widetilde{R} \\ f &= 2x_k^T \widetilde{A}^T \widetilde{Q} \widetilde{B} \end{aligned} \tag{18b}$$

Therefore, the objective function is transformed into a function with only one variable U, and then we can find the extreme value of the function J to obtain the optimal control quantity.

To summarize the above formula derivation, it is essentially divided into two steps: the variable replacement of the future state quantity and the transformation of the optimization objective function.

4. Particle Swarm Optimization

In the early stage of the study, scholars observed and studied birds' predation behaviors. In 1995, Kennedy and Eberhart [26] proposed the particle swarm optimization algorithm. When birds hunt for food, they search in the simplest and most effective way. Each food in PSO represents a feasible solution, and each feasible solution corresponds to a fitness value, which is used as the basis for judging the merits of the solution. The fitness value is determined by the particle itself and the defined fitness function.

In a D-dimensional search space, a population is composed of N particles, where the position of the ith particle in the D-dimensional space is denoted by $X_i = (x_{i1}, x_{i2}, \cdots x_{iD})^T$. The corresponding fitness value is calculated by the objective function and the position coordinate of the current ith particle. In the process of iteration, the velocity and position of the particles are updated by the iterative formula, and then the individual extreme value and the group extreme value are updated to obtain the next generation of particles, so as to find the global optimal solution.

$$V_{id}^{k+1} = \omega V_{id}^k + c_1 r_1 (P_{id}^k - X_{id}^k) + c_2 r_2 (P_{gd}^k - X_{id}^k) \tag{19a}$$

$$X_{id}^{k+1} = X_{id}^k + V_{id}^{k+1} \tag{19b}$$

where ω is the inertia weight of the velocity, which represents the ability of the particle to inherit the velocity of the particle in the previous step; c_1 and c_2 are non-negative constants, e.g., the acceleration factor; r_1 and r_2 are constants belonging to [0, 1]. $d = 1, 2 \cdots D$; v_{id}^{t+1} and x_{id}^{t+1} refer to the velocity and position of the d dimension of the ith particle in the $(t + 1)$ iteration, respectively; $pbest_{id}^t$ denotes the individual extremum of the ith particle in the d dimension; and $gbest_d^t$ denotes the global extremum of the group in the d dimension.

The algorithm process is detailed in steps as follows:

Step 1: Initialize the swarm particles, set the initialization parameters and fitness function, and randomly generate the position and velocity of all particles.

Step 2: Calculate each particle's fitness value through the fitness function according to its own parameters, which is used as the selection standard.

Step 3: Select the optimal particle according to the fitness value of each particle as the individual extreme value and the group extreme value.

Step 4: Update the particle velocity and position by iteratively updating Equations (19a) and (19b).

Step 5: Determine the termination condition (usually set as the maximum number of iterations or the upper and lower limits of fitness value). If it is satisfied, perform Step 6; otherwise, perform Step 2.

Step 6: Output the global optimal solution.

5. PSO-Based Model Predictive Control

To solve the problem of maximizing the objective function of the equation, in this paper, we propose a model predictive control strategy based on particle swarm optimization to optimize the iterative optimization process of the system. The strategy is essentially divided into the following steps: initializing the system parameters and setting the system

objective function; calculating the individual extreme value and group extreme value of the current particle swarm; and obtaining the optimal solution of the system control input by searching in the global area. The optimal control solution was substituted into the MPC model for steady-state adjustment. The optimal control procession tuned using intelligent algorithms is shown in Figure 3.

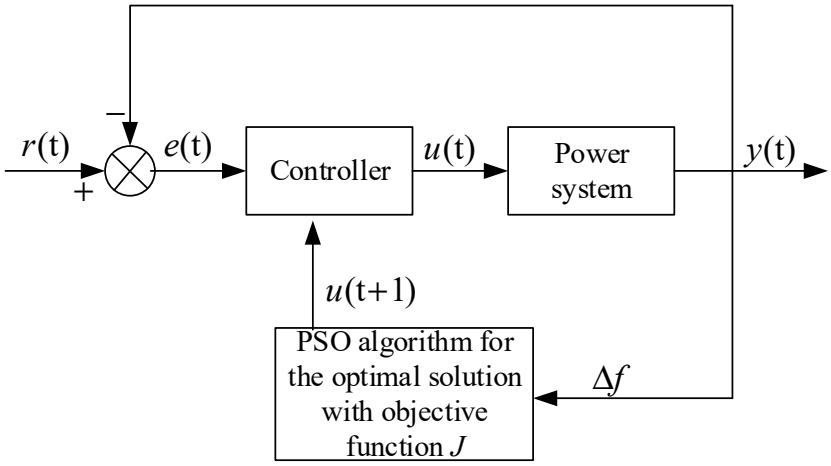

Figure 3. PSO-MPC of the power system.

Here, we add constraints into the control:

$$u_{\min} \leq u(k) \leq u_{\max}$$

To facilitate the implementation of the proposed MPC strategy based on PSO optimization, the three steps discussed above are summarized in the flowchart shown in Figure 4.

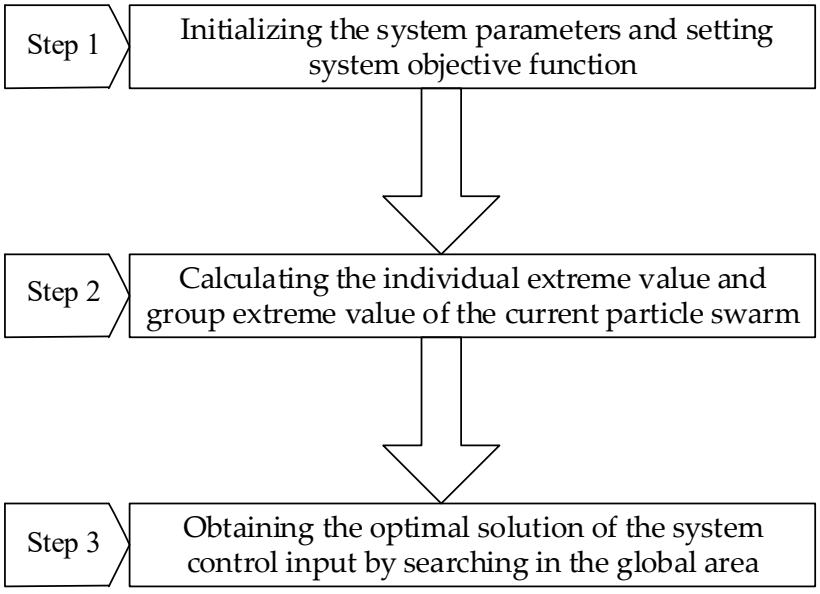

Figure 4. Flowchart of the proposed PSO-MPC.

The initialization process is as follows (Algorithm 1):

Algorithm 1 Require: N_u, *ger*

for $i = 1 \rightarrow$ ger do
for each particle $u_i \in N_u$ do
Initialize u_i with a uniformly random distribution in the search space considering the limitation (18a) and (18b) (Initialize each particle)
end for
$pbest\_u \leftarrow u_i$ (Initialize personal best solution)
if $J(pbest\_u) < J(pbest\_u)$ then
$gbest\_u \leftarrow pbest\_u$ (Initialize globe best solution, J is cost function (17a))
end if
end for

The PSO optimization process is as follows (Algorithm 2):

Algorithm 2 Require: *ger*, *k*

for $j = 1 \rightarrow k$ do
for $i = 1 \rightarrow ger$ do
if $J(u_i) < J(pbest\_u)$ then
$pbest\_u \leftarrow u_i$
end if
if $J(pbest\_u) < J(gbest\_u)$ then
$gbest\_u \leftarrow pbest\_u$
end if
end for
$x(k+1) = Ax(k) + Bgbest(k) + Cz(k)$
end for

In the whole iterative optimization process, the cost function J is used as the fitness function of the PSO optimization algorithm, the fitness value of the control variables u of the system is calculated under the constraints, and the minimum value of the fitness value is assigned to the individual optimal value and the group optimal value to obtain $u(k+1) = gbest\_u$. The velocity and position are updated by Equations (19a) and (19b), and a new round of fitness value calculations occurs.

6. Simulation and Discussion

Because of the powerful calculation and programming functions of MATLAB, it is widely used in mathematical modeling and simulation control. In this study, we used MATLAB 2019a to validate the effectiveness of the PSO-MPC control strategy with wind turbines. The specific system parameters are shown in Table 2.

Table 2. Model parameters of the power system with wind turbines.

D = 0.389 pu/Hz	$w_{opt} = 1.15$ rad/s
R = 0.04 Hz/pu	$R_r = 0.00552$ pu
$T_t = 0.355$	$R_s = 0.00491$ pu
$T_g = 0.806$	$H_t = 4.5$ pu
H = 12 pu·s	$L_r = 0.1$ H
$\beta = 1$	$L_s = 0.09273$ H
	$L_m = 3.9654$ H

Here, we provide the parameter settings of the PSO-MPC controller. According to Equations (19a) and (19b), the parameter settings of the particle swarm optimization method are given as follows: according to $u = \begin{bmatrix} \Delta P_c & \Delta V_{qr} \end{bmatrix}^T$, the feasible solution dimension $d = 2$, the maximum number of iterations $ger = 100$, the particle position parameter limit

corresponding to MPC controller control quantity u) $u_{min} = -0.5$, $u_{max} = 0.5$, the velocity limit $v_{min} = -0.5$, $v_{max} = 0.5$, the inertia weight w = 0.8, the individual acceleration factor $c_1 = 0.5$, and the group acceleration factor $c_2 = 0.5$.

According to Equation (16a), the parameter settings of the model prediction controller are given as follows: the prediction horizon N_p = 10, the control horizon N_c = 10, the weight parameters Q = diag(100,0,0,100,0) and R = diag(1,0), and the sampling time was chosen as 0.2 s.

6.1. Comparison with Different Load Disturbance Values

To verify the dynamic performance of the system, two kinds of load disturbance values were respectively used to verify the system strategy: $\Delta P_{L1} = 0.02 * (rand(1) - 0.5)$ and $\Delta P_{L2} = 0.04 * (rand(1) - 0.5)$.

Figure 5 gives the dynamic response curve of the load frequency deviation under the PSO-MPC strategy with wind turbines. Figure 5a is the dynamic response curve of the load frequency deviation under load disturbance $\Delta P_{L1} = 0.02 * (rand(1) - 0.5)$. Figure 5b is the dynamic response curve of the load frequency deviation under load disturbance $\Delta P_{L2} = 0.04 * (rand(1) - 0.5)$. As can be seen from the frequency response during random load disturbances, the load frequency deviation of the power system can quickly converge to zero using the proposed PSO-MPC. This fully proves the effectiveness of the PSO-MPC strategy designed in this paper, and the feasibility of involving wind turbines in frequency regulation.

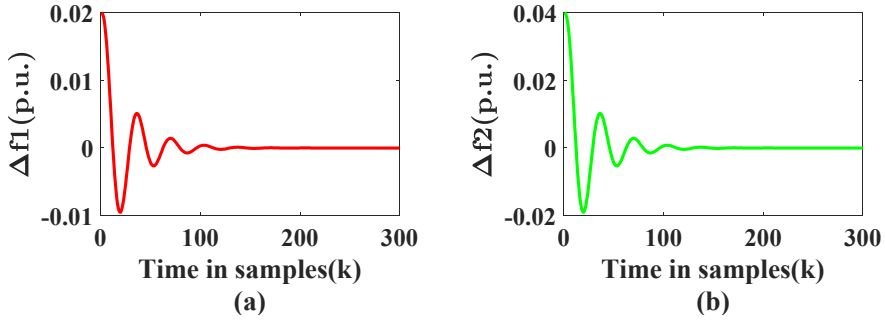

Figure 5. Dynamic response curve of the load frequency deviation under the PSO-MPC strategy with wind turbines. (**a**) Load frequency deviation under ΔP_{L1}; (**b**) Load frequency deviation under ΔP_{L2}.

Figure 6 illustrates the dynamic response curve of the wind turbine output power deviation signal ΔP_e under the PSO-MPC strategy with wind turbines. Among them, Figure 6a,b both rapidly converge to zero after experiencing transient fluctuations under two kinds of disturbances. This verifies the feasibility of using wind turbines as a supplement to traditional power generation strategies.

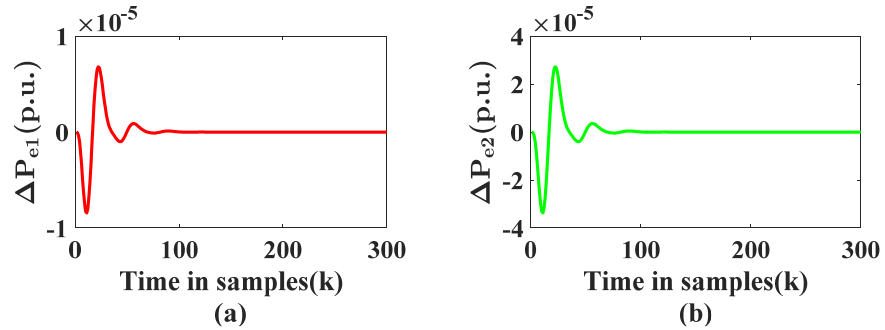

Figure 6. Output power deviation signal ΔP_e of wind turbines under the PSO-MPC strategy with wind turbines. (**a**) Output power deviation under ΔP_{L1}; (**b**) Output power deviation under ΔP_{L2}.

Figure 7 demonstrates the dynamic response curve of the control input signal ΔP_c of the traditional generator under the PSO-MPC strategy with the participation of wind turbines. According to the dynamic response curves of Figure 7a,b under two kinds of disturbances, it can be seen that the first control component of the designed PSO-MPC strategy can converge to zero after a short adjustment.

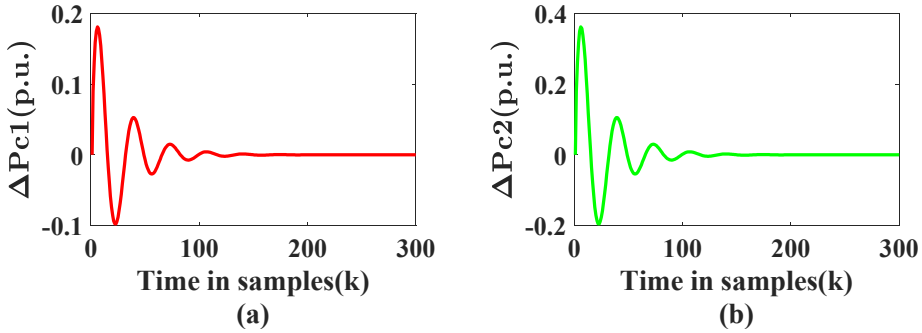

Figure 7. Control input signals ΔP_c under the PSO-MPC strategy with wind turbines. (**a**) Control input under ΔP_{L1}; (**b**) Control input under ΔP_{L2}.

Similarly, the output deviation of the governor and the output deviation of the valve body of the traditional generator set under the PSO-MPC strategy with the participation of the wind turbines are given in Figures 8 and 9. In the case of experiencing two kinds of disturbances, both converge to zero after a short fluctuation adjustment. This verifies the feasibility of applying the PSO-MPC strategy in a traditional generator set control.

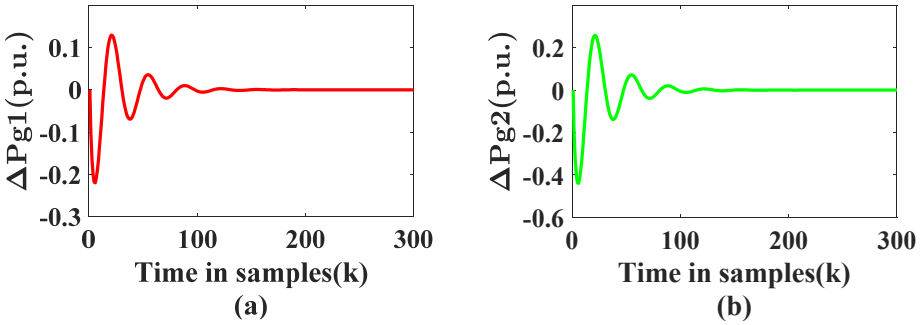

Figure 8. Output deviation signal of governor ΔP_g under the PSO-MPC strategy with wind turbines. (**a**) Output deviation signal of governor ΔP_g under ΔP_{L1}; (**b**) Output deviation signal of governor ΔP_g under ΔP_{L2}.

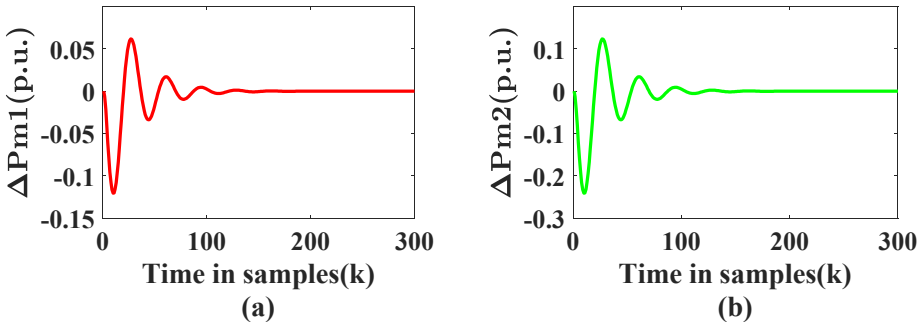

Figure 9. Output deviation signal of turbine body ΔP_m under the PSO-MPC strategy with wind turbines. (**a**) Output deviation signal of turbine body ΔP_m under ΔP_{L1}; (**b**) Output deviation signal of turbine body ΔP_m under ΔP_{L2}.

Figure 10 demonstrates the dynamic response curve of the wind turbine's control input signal based on a doubly fed induction machine under the PSO-MPC strategy. Under $\Delta P_{L1} = 0.02$ (Figure 10a) and $\Delta P_{L2} = 0.04$ (Figure 10b) disturbances, the second control component ΔV_{qr} of the designed PSO-MPC strategy can converge to zero, and the convergence velocity is faster than that of the first control component ΔP_c.

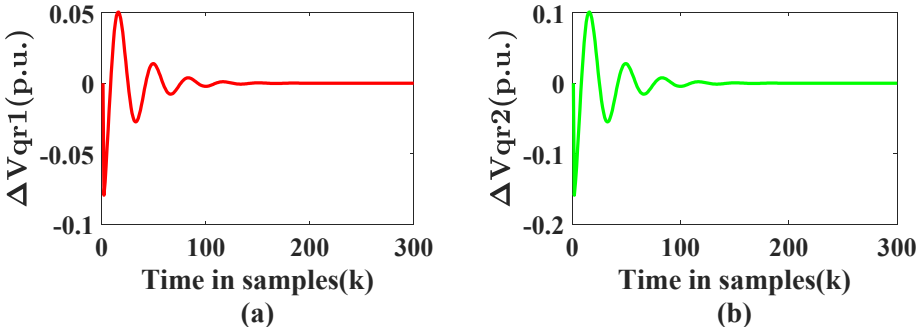

Figure 10. Control input signal ΔV_{qr} under the PSO-MPC strategy with wind turbines. (**a**) Control input signal ΔV_{qr} under ΔP_{L1}; (**b**) Control input signal ΔV_{qr} under ΔP_{L2}.

6.2. Comparison with Control Methods

To verify the dynamic performance of the system, the results of the MPC, PSO-PID, and PSO-MPC algorithms were compared. Under $\Delta P_L = 0.02 * (rand(1) - 0.5)$ disturbance, and the same system parameters, the simulation results were as follows:

Figure 11 shows the system response curves of the load frequency deviation under three strategies with wind turbines. Under $\Delta P_L = 0.02$ disturbance, it can be seen that the load frequency deviation under the PSO-MPC strategy exhibited a smaller overshoot and reached stability more quickly as compared with the MPC and PSO-PID control strategies. This fully proves the effectiveness of the PSO-MPC strategy designed in this paper, and the feasibility of involving wind turbines in frequency regulation.

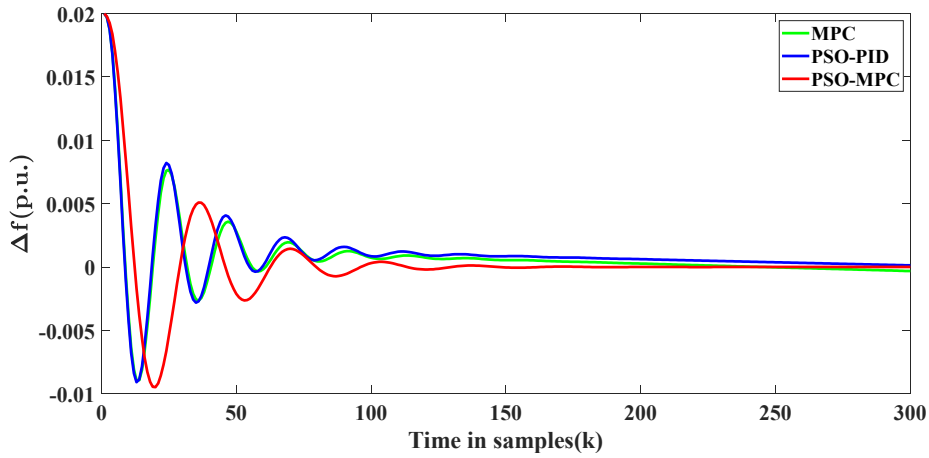

Figure 11. Dynamic response curve of the load frequency deviation under the three strategies with wind turbines.

Similarly, Figures 12 and 13 show the output deviation signal of the governor and turbine body under three strategies with wind turbines. Under the MPC, PSO-PID, and PSO-MPC control strategies, the overshoots of the MPC and PSO-PID control strategies were larger than that of the PSO-MPC control strategy. In terms of convergence, PSO-MPC exhibited a faster convergence velocity and better stability performance.

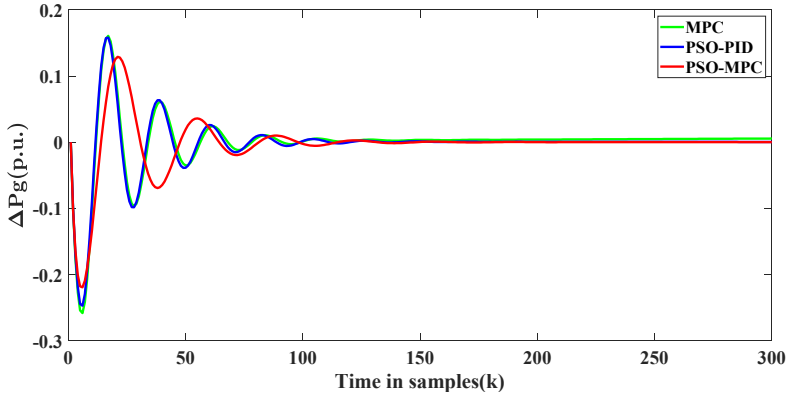

Figure 12. Output deviation signal of the governor ΔP_g under the three strategies with wind turbines.

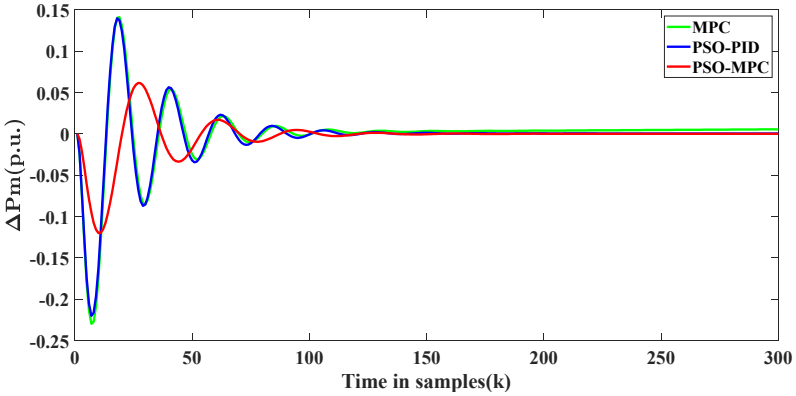

Figure 13. Output deviation signal of the turbine body ΔP_m under the three strategies with wind turbines.

7. Conclusions

In this paper, we propose a particle swarm optimization-based model predictive control (PSO-MPC) strategy for the load frequency control of a hybrid power system integrated with wind turbines. Aiming to solve the problems of the uncertainty of wind turbines and the heavy computation of the MPC strategy, we propose an MPC strategy for LFC with wind turbines based on the particle swarm optimization algorithm. Under the proposed PSO-MPC control strategy, the load frequency performed better in view of the large disturbances and strong levels of uncertainty associated with wind turbines. Moreover, in the iterative optimization process of MPC, LFC improves the time of the controller fluctuation adjustment and the burden of calculation and communication. The simulation results show that the proposed PSO-MPC strategy can quickly adjust the fluctuations caused by the disturbance and effectively converge to zero after a short overshoot period.

In addition, the comparisons of the three control strategies, namely, MPC, PSO-PID, and PSO-MPC, show that the proposed PSO-MPC control strategy significantly improves the frequency stability of the system. Furthermore, the overshoot of the system response was reduced, producing a more stable performance. Through the above simulation results, it is verified that the PSO-MPC strategy proposed in this paper exhibits good performance in terms of load frequency control with the participation of wind turbines. The strategy overcomes the problems of slow response, large fluctuations, and low fault tolerance associated with traditional control methods.

Since parameters such as learning factors are fixed values in the PSO algorithm, the optimal solution may be missed in the late iteration stage because of the large update step. In this case, the control strategy may result in a slow iterative operation or produce the local optimal solution problem. In the future, more general power generation systems with parameter uncertainties will be explored, and the applicability of neural networks with the MPC strategy will be tested.

Funding: This research received no external funding.

Data Availability Statement: Not applicable.

Conflicts of Interest: The authors declare no conflict of interest.

References

1. Sharma, Y.; Saikia, L.C. Automatic generation control of a multi-area ST—Thermal power system using Grey Wolf Optimizer algorithm based classical controllers. *Int. J. Electr. Power Energy Syst.* **2015**, *73*, 853–862. [CrossRef]
2. Delassi, A.; Arif, S.; Mokrani, L. Load Frequency Control Problem in Interconnected Power Systems Using Robust Fractional PIλ D Controller. *Ain Shams Eng. J.* **2018**, *9*, 77–88. [CrossRef]
3. Rana, K.; Kakran, S. Improvement in dynamic performance of an interconnected power system in LFC using PID and fuzzy controller. In Proceedings of the 2016 International Conference on Emerging Trends in Electrical Electronics & Sustainable Energy Systems (ICETEESES), Sultanpur, India, 11–12 March 2016; pp. 25–29.
4. Mewara, A.; Parmar, G. Comparison of DE optimized PID controllers for AGC of interconnected power system. In Proceedings of the 2017 International Conference on Computer, Communications and Electronics (Comptelix), Jaipur, India, 1–2 July 2017; pp. 178–182.
5. Islam, S.; el Saddik, A.; Sunda-Meya, A. Robust cooperative load-frequency tracking protocols for leader-follower smart power grid networks with uncertainty. In Proceedings of the 2019 IEEE International Conference on Systems, Man and Cybernetics (SMC), Bari, Italy, 6–9 October 2019; pp. 1794–1800.
6. Zhang, K.; Zhou, B.; Zheng, W.X.; Duan, G.-R. Event-Triggered and Self-Triggered Gain Scheduled Control of Linear Systems with Input Constraints. *IEEE Trans. Syst. Man Cybern. Syst.* **2022**, *52*, 6452–6463. [CrossRef]
7. Hu, Z.; Liu, S.; Yang, L.; Wu, L. Distributed fuzzy filtering for load frequency control of non-linear interconnected power systems under cyber-physical attacks. *IET Control Theory Appl.* **2020**, *14*, 527–538. [CrossRef]
8. Hamida, H.; Kilani, K.B.; Elleuch, M. Implementation of LFC based fuzzy logic controller for the tunisian power system. In Proceedings of the 2018 15th International Multi-Conference on Systems, Signals & Devices (SSD), Yasmine Hammamet, Tunisia, 19–22 March 2018; pp. 508–513.
9. Hu, Z.; Liu, S.; Luo, W.; Wu, L. Resilient Distributed Fuzzy Load Frequency Regulation for Power Systems Under Cross-Layer Random Denial-of-Service Attacks. *IEEE Trans. Cybern.* **2020**, *52*, 2396–2406. [CrossRef] [PubMed]
10. Magzoub, M.A.; Alquthami, T. Optimal Design of Automatic Generation Control Based on Simulated Annealing in Interconnected Two-Area Power System Using Hybrid PID—Fuzzy Control. *Energies* **2022**, *15*, 1540. [CrossRef]
11. Abhayadev, S.; Ramesh Kumar, P. Effect of DFIG wind turbines on LFC in a sliding mode controlled power system. In Proceedings of the 2021 6th International Conference for Convergence in Technology (I2CT), Maharashtra, India, 2–4 April 2021; pp. 1–6.
12. El-Saady, G.; Youssef, A.M.; Ibrahim, E.N.M.; Nour-Eldin, S.A. Effect of wind driven double-fed induction generator upon the stability of decentralized power systems via load frequency controllers design. In Proceedings of the 2019 21st International Middle East Power Systems Conference (MEPCON), Cairo, Egypt, 17–19 December 2019; pp. 803–808.
13. Sun, X.; Liao, K.; Yang, J.; He, Z. Model predictive control based load frequency control for power systems with wind turbine generators. In Proceedings of the 2019 IEEE Innovative Smart Grid Technologies—Asia (ISGT Asia), Chengdu, China, 21–24 May 2019; pp. 1387–1392.
14. Mahdi, M.M.; Thajeel, E.M.; Ahmad, A.Z. Load frequency control for hybrid micro-grid using MRAC with ANN under-sudden load changes. In Proceedings of the 2018 Third Scientific Conference of Electrical Engineering (SCEE), Baghdad, Iraq, 19–20 December 2018; pp. 220–225.
15. Veerasamy, V.; Wahab, N.I.A.; Ramachandran, R.; Othman, M.L.; Hizam, H.; Irudayaraj, A.X.R.; Guerrero, J.M.; Kumar, J.S. A Hankel Matrix Based Reduced Order Model for Stability Analysis of Hybrid Power System Using PSO-GSA Optimized Cascade PI-PD Controller for Automatic Load Frequency Control. *IEEE Access* **2020**, *8*, 71422–71446. [CrossRef]
16. Sundararaju, N.; Vinayagam, A.; Veerasamy, V.; Subramaniam, G. A Chaotic Search-Based Hybrid Optimization Technique for Automatic Load Frequency Control of a Renewable Energy Integrated Power System. *Sustainability* **2022**, *14*, 5668. [CrossRef]
17. Hu, Z.; Liu, S.; Wu, L. Credibility-based distributed frequency estimation for plug-in electric vehicles participating in load frequency control. *Int. J. Electr. Power Energy Syst.* **2021**, *130*, 106997. [CrossRef]
18. Behara, R.K.; Saha, A.K. Artificial Intelligence Control System Applied in Smart Grid Integrated Doubly Fed Induction Generator-Based Wind Turbine: A Review. *Energies* **2022**, *15*, 6488. [CrossRef]
19. Yan, Z.; Xu, Y. A Multi-Agent Deep Reinforcement Learning Method for Cooperative Load Frequency Control of a Multi-Area Power System. *IEEE Trans. Power Syst.* **2020**, *35*, 4599–4608. [CrossRef]
20. Chien, T.-H.; Huang, Y.-C.; Hsu, Y.-Y. Neural Network-Based Supplementary Frequency Controller for a DFIG Wind Farm. *Energies* **2020**, *13*, 5320. [CrossRef]
21. Hu, Z.; Liu, S.; Luo, W.; Wu, L. Intrusion-Detector-Dependent Distributed Economic Model Predictive Control for Load Frequency Regulation with PEVs Under Cyber Attacks. *IEEE Trans. Circuits Syst. I Regul. Pap.* **2021**, *68*, 3857–3868. [CrossRef]
22. Ali, A.; Khan, B.; Mehmood, C.A.; Ullah, Z.; Ali, S.M.; Ullah, R. Decentralized MPC based frequency control for smart grid. In Proceedings of the 2017 International Conference on Energy Conservation and Efficiency (ICECE), Lahore, Pakistan, 22–23 November 2017; pp. 1–6.

23. Kunya, A.B.; Argin, M.; Kucuksari, S. Optimal load frequency control of multi-area power system considering incremental control action. In Proceedings of the 2019 IEEE Texas Power and Energy Conference (TPEC), College Station, TX, USA, 7–8 February 2019; pp. 1–6.
24. Rehiara, A.B.; Chongkai, H.; Sasaki, Y.; Yorino, N.; Zoka, Y. An adaptive IMC-MPC controller for improving LFC performance. In Proceedings of the 2017 IEEE Innovative Smart Grid Technologies-Asia (ISGT-Asia), Auckland, New Zealand, 4–7 December 2017; pp. 1–6.
25. Uyioghosa, I.E.; Saha, A.K. DMPC scheme for load frequency control with application to interconnected power system. In Proceedings of the 2020 International SAUPEC/RobMech/PRASA Conference, Cape Town, South Africa, 29–31 January 2020; pp. 1–6.
26. Kennedy, J.; Eberhart, R.C. Particle swarm optimization. In Proceedings of the IEEE International Conference on Neural Networks, Perth, WA, Australia, 27 November–1 December 1995; Volume 4, pp. 1942–1948.
27. Redoy, M.S.; Ruma. Load Frequency control of an inter connected power system using PSO based PID controller. In Proceedings of the 2022 International Conference on Advancement in Electrical and Electronic Engineering (ICAEEE), Gazipur, Bangladesh, 24–26 February 2022; pp. 1–5.
28. Xu, Z.; Wang, D.; Yi, G.; Hu, Z. Asynchronous Tracking Control of Amplitude Signals in Vibratory Gyroscopes with Partially Unknown Mode Information. *IEEE Trans. Ind. Electron.* **2022**. [CrossRef]
29. Veerasamy, V.; Wahab, N.I.A.; Ramachandran, R.; Vinayagam, A.; Othman, M.L.; Hizam, H.; Satheeshkumar, J. Automatic Load Frequency Control of a Multi-Area Dynamic Interconnected Power System Using a Hybrid PSO-GSA-Tuned PID Controller. *Sustainability* **2019**, *11*, 6908. [CrossRef]
30. Veerasamy, V.; Wahab, N.I.A.; Ramachandran, R.; Othman, M.L.; Hizam, H.; Kumar, J.S.; Irudayaraj, A.X.R. Design of single- and multi-loop self-adaptive PID controller using heuristic based recurrent neural network for ALFC of hybrid power system. *Expert Syst. Appl.* **2021**, *192*, 116402. [CrossRef]
31. Al-Majidi, S.D.; Al-Nussairi, M.K.; Mohammed, A.J.; Dakhil, A.M.; Abbod, M.F.; Al-Raweshidy, H.S. Design of a Load Frequency Controller Based on an Optimal Neural Network. *Energies* **2022**, *15*, 6223. [CrossRef]
32. Jin, X.; Tan, W.; Zou, Y.; Wang, Z. Active Disturbance Rejection Control for Wind Turbine Fatigue Load. *Energies* **2022**, *15*, 6178. [CrossRef]